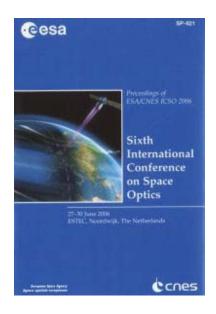# International Conference on Space Optics—ICSO 2006

Noordwijk, Netherlands

27–30 June 2006

Edited by Errico Armandillo, Josiane Costeraste, and Nikos Karafolas

Numerical line of sight stabilisation for high resolution earth observation from high orbits

P. Blanc, G. Monroig

NUMERICAL LINE OF SIGHT STABILISATION FOR HIGH RESOLUTION EARTH OBSERVATION FROM HIGH ORBITS

Blanc P., Monroig G.

Alcatel Alenia Space,100 Bd. du Midi, B.P. 99 F-06156 Cannes La Bocca, France
Email: philippe.blanc@alcatelaleniaspace.com

ABSTRACT

Controlling line of sight instabilities due to platform μ-vibrations is a major issue for High Orbits (HO) decametric and metric Earth Observation imaging systems. Indeed, as image quality is strongly impacted by such μ-vibrations during integration time, observation from HO requires a very high angular precision around tens of millirad over tens or even hundreds of milliseconds. This angular stability requirement is out of scope for conventional Attitude and Orbit Control System (AOCS). Two different solutions – post-accumulation and closed-loop control of the line of sight – are envisaged and discussed to deal with those μ-vibrations to make possible decametric or metric Earth Observation from High Orbits.

1. INTRODUCTION

Permanent High Resolution observation and instant accessibility are the main advantages of metric and decametric imaging systems from High Orbits (e.g. Geostationary).

Such imaging systems require the use of very large diameter telescopes, technically unfeasible with standard monolithic concepts. Accordingly, multi-pupils instruments have been studied in order to make such missions feasible. Different instrument concepts based on Optical Aperture Synthesis (OAS) have been proposed ([2],[4],[5]) and, in this paper we mainly focus on the OAS 1,2 meter resolution Geo imaging instrument consisting of nine 1,8 m diameter pupils as described in [4]. As a comparison, we also consider the – unfeasible – 16 m diameter monolithic instrument that was used as an Image Quality (IQ) reference in this study.

One of the major issues that has raised in those studies is the line of sight μ-vibrations during the integration time.

Indeed, the line of sight instabilities can imply image blurring characterized by a degradation of the Optical Transfer Function (OTF) of the imaging system.

In [7], Stern and Kopeika show that the OTF degradation due to motion blur is the Fourier transform of the probability-density function (PDF) of the line of sight ground location during the integration time. The Fig. 1 shows that the OTF degradation implied by μ-vibrations depends on the corresponding maximum displacements during the integration time and also on the type of the μ-vibration characterized by its PDF.
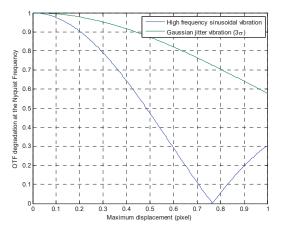

Fig. 1. OTF degradations at the Nyquist freq. *v.s.* maximum displacement for high frequency sinusoidal and Gaussian jitter vibrations.

For an optical imaging system, a typical admissible OTF degradation at the Nyquist frequency of 0.9 implies a line of sight stability requirement during the integration time of approximately 1/10 pixel RMS.

From the Geostationary orbit (36000 km), the pixel based accuracy requirement results in a very high angular precision. For example, a 1 m RMS ground stability implies a 30 nrad angular precision for the platform attitude.

Second, as the instantaneous field of view (IFOV) is small for HR observation from High Orbit, typical required integration times are over than tens of milliseconds for monolithic or deployable primary mirror instruments, or even hundreds of milliseconds for OAS instruments.

The Table 1 shows typical required angular stability and integration time for different Geo HR imaging systems.

Table 1. Typical required angular stability and integration time for different Geo HR imaging systems.

	GSD[*]	Angular accuracy (RMS)	Integration time
9-pupil OAS system	1.2 m	3.5 nrad	250 ms
mono-pupil system	1.2 m	3.5 nrad	3 ms
segmented mono-pupil system (5 m)	5 m	14 nrad	3 ms

[*] *GSD : Ground Sampling Distance*

Angular accuracy and integration time requirement for HR imaging systems in LEO is about hundreds of nrad over less than 1 ms: the line of sight stability requirements are relaxed in the order of magnitude of one to three, compared to the Geo HR instruments.

Obviously, such angular attitude accuracies over tens or even hundreds of milliseconds are out of scope of the AOCS generally limited by the accuracy and the bandwidth of attitude sensors and actuators.

To make possible decametric and metric Earth Observation from high orbits, two solutions – post-accumulation *(§2)* and closed-loop control of the line of sight *(§3)* – are presented and discussed in this paper to deal with those μ-vibrations of the line of sight.

2. POST-ACCUMULATION

It is first considered to divide the acquisition time into many elementary smaller acquisition periods. It provides a multi-image frame instead of a "simple" image of the scene. The integration time of each elementary acquisition, noted hereinafter Ti^*, is chosen short enough to consider the μ-vibrations amplitude to be compliant with the line of sight stability requirement. So, the goal of post-accumulation is to "freeze" the μ-vibrations during each short integration time acquisitions and to use each of these short exposure images for incrementally constructing the final image.

To do that, the average of the N acquired images is computed after a sub-pixel accuracy numeric co-registration post-processing. This algorithm provides an estimation of the geometric disparity between the current image and the first image chosen as the reference image. Then, the current image is resampled with the estimated translation.

The co-registration estimation, based on standard sub-pixel correlation registration method [6], is here applied in a very favourable case where the geometric disparity is a simple translation estimated with a very large number of pixels. The standard deviation of the error of this estimation is inversely proportional to the Signal to Noise Ratio (SNR) per pixel, the square root of the

number of pixels and also to a term of contrast depending on the OTF and on the image itself [3].

For example, two raw images with very low SNR provided by the 9-pupil OAS system, such as the one depicted by the Fig. 2, can be co-registered with a sub-pixel accuracy better than 1/50 pixel RMS, assuming at least 512x512 pixels sub-images are used in the correlation registration algorithm.
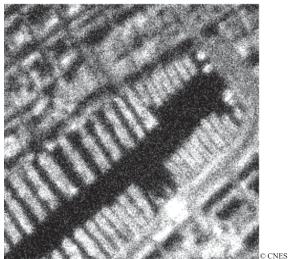

© CNES

Fig. 2. Simulated 512x512 raw image from the 9-pupil OAS system with a 2 ms integration time (SNR = 5).

Instead of "simply" computing the average of the co-registered images, it is possible to take advantage of the μ-vibrations to apply a super-resolution algorithm. Indeed, each image of the multi-image frame is the result of the same sampling grid but randomly translated. Therefore, by analysing those sub-pixel translations between the different images, it is possible to generate a "super-resolved" image with a better sampling ground distance, typically up to a factor two.

However, as super-resolution algorithm relies on aliasing in raw images, this processing is the more efficient as the optical cut-off frequency of the telescope is greater than the Nyquist frequency. Thus, the super-resolution algorithm is not really applicable for the 9-pupil OAS system, whose Nyquist frequency to optical cut-off frequency ratio is about 0.98. On the other hand, its application would be interesting for the 16 m monolithic system whose ratio is about 0.62.

The main drawback – and limitation – of the post-accumulation is that the number of images can be very important as the elementary integration time Ti^* is small. The Fig. 3 shows, in log-scale, the required number of images versus Ti^* for the 9-pupil OAS system. Owing to preliminary μ-vibrations studies, an integration time of 2 ms is compliant with the line of

sight stability requirements: therefore, in this case the post-accumulation would require about 800 elementary images.
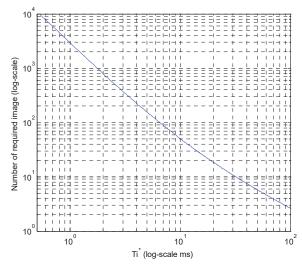

Fig. 3. Number of required elementary images for post-accumulation versus the elementary integration time.

This potentially huge number of images for the post-accumulation processing raises up two main issues.

First, there is a fixed time gap (read-out time) of tens of milliseconds between two elementary acquisitions, necessary to the data transfer into the mass memory. Therefore, instead of a 250 ms integration time, post-accumulation implies tens of seconds or even minutes between the first and the last elementary acquisitions, raising up the issue of moving objects in the scene (e.g. cars, trucks, ...). A specific algorithm has to be developed to handle correctly those moving objects during the post-accumulation processing.

Second, as the resampling processing – and *a fortiori* the super-resolution algorithm – applied to images with typically hundreds of Mpixels is very time and memory consuming, the post-accumulation leads to possible prohibitive data transfer and memory problems.

3. CLOSED-LOOP CONTROL OF THE LINE OF SIGHT

It is the reason why we plan to study an active closed-loop control of the line of sight. The perturbations due to μ-vibrations are measured thanks to a real time numeric analysis of a high rate image frame provided by small CMOS matrices on the focal plane and the actuations are provided by a fast steering mirror (FSM).

3.1 Typical vibrations to damp

Typical line of sight instabilities, due to plat-form μ-vibrations, are constituted of:
• low frequency vibrations ([0-1] Hz) mainly due to AOCS residues;
• high frequency sinusoidal vibrations due to AOCS actuators. Reaction wheels, for instance, generate vibrations at the rotation frequency of the wheel and at higher harmonics.

Our aim is to efficiently damp line of sight μ-vibrations, up to the pixel accuracy of 1/10 pixel RMS. To this end, we consider a vibrations sensor and an actuator controlled in a closed-loop. The closed-loop control is meant to uncouple the instrument and the plat-form, as far as μ-vibrations are concerned.

3.2 Principle of the closed-loop control

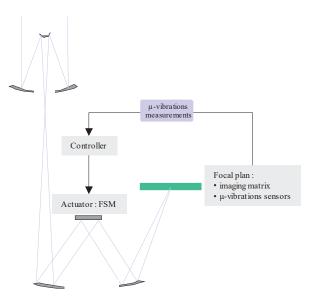The scheme of the closed-loop control is presented in Fig. 4:

Fig. 4. The general closed-loop scheme

Let us detail the components of the closed-loop control:

▪ **μ-vibrations sensor:**
This sensor is high temporal rate small CMOS matrices combined with an on-board real-time numeric correlation algorithm: the current small image is compared to a reference image to supply an estimate of the tip-tilt line of sight displacement. As shown in the Fig. 5, the matrices are positioned in periphery of the main imaging matrix.
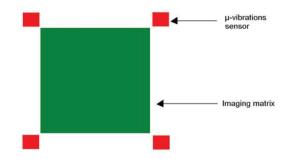
Fig. 5. Example of an arrangement of the sensors on the focal plane.

There are two major advantages to this structure: such a sensor directly provides a measurement of the displacement without relative variations, because the small matrices are closely positioned around the imaging matrix. Besides, as those sensors observe the Earth with the same optical instrument as the imaging matrix, it has the same μ-vibrations sensitivity, but at a much higher temporal rate and with a worst SNR per pixel. On top of that, those sensors are quite "simple" and do not require any additional complex optical nor mechanical sub-systems dedicated to vibrations measurement, such as accelerometers.

As previously stated in §2, the standard deviation of the error of inter-image translation measurement decreases with the increase of the integration time (Ti) *via* the SNR that takes into account photonic and read-out noises, and of the square root of the number of pixels of the small matrices (Np):

$$\sigma_e = \left(SNR(Ti).\sqrt{Np}.Contrast \right)^{-1} \qquad (1)$$

As the sensor's accuracy is locally image-dependent (contrast term), to maximise the probability to find a contrasted scene in the small matrix's FOV, it is wise to use several sensors. Moreover, in addition to the translation measurement, it is possible to estimate its confident interval and, thus, to resort to a multi-sensor fusion algorithm meant to provide robust translation measurements.

Finally, the sensor response time Tr is equal to the sum of the integration time Ti, the matrix read-out time and the computation time necessary to calculate the displacement. The read-out time depends on the number of pixels and on the bus rate. The computation time depends on the number of pixels, the square of the research area and on the on-board processor's speed, expressed in Million of Instructions Per Second (MIPS).

Thus, a compromise between measurement quality and frequency must be adopted.

For instance, if we consider a pixel bus rate of 25 Mpixel/s, a 2100 MIPS processor (e.g. POWERPC) and a research area of 2 pixels and a required measurement precision of a 1/20 pixel RMS, then we obtain results synthesized in the Table 2 and illustrated by the Fig. 6.

Table 2. Main features and performance of the μ-vibrations sensors for the two HR Geo imaging systems.

	Matrix size	integration time	Measurement Freq. (1/Tr)
9-pupil OAS system	112x112	3 ms	180-220 Hz
mono-pupil system	64x64	0.2 ms	1000-1300 Hz

In the two previous examples, the lower measurement frequency is obtained with a registration by correlation algorithm, while the higher is obtained with a more efficient registration algorithm.
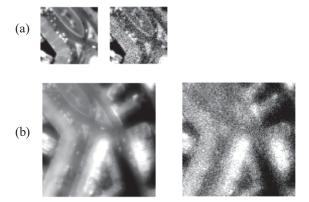
(a)

(b)

Fig. 6. Examples of images acquired by the 64x64 pixels sensor (a) and 112x112 pixels sensor (b), respectively with and without the detection noise.

▪ **Controller:**
The controller is particularly efficient in damping low frequency vibrations and becomes less and less effective as the vibration frequency increases. A corrector has a limit frequency beyond which vibrations are not damped enough. This frequency is determined by the required damping, the sampling frequency and the controller itself.

▪ **Actuator:**
A fast steering mirror is used. It is a very good resolution Tip-Tilt mirror, itself under a closed-loop control. It has a cut-off frequency around 100-200 Hz, decreasing with the increase of the size of the mirror.

As far as optical design is concerned, the FSM must be situated in a real image plane. An example of optical design is presented in the Fig. 8 of [4]. In order to get a global image translation, the FSM is placed on the real exit pupil. The distance between the mirror and the focal plane is d=7891 mm and the FSM diameter is 230 mm.

A resolution of 1/10 pixel (13x13 μm^2) leads to a resolution on the angle equal to 80 nrad. This seems to be too ambitious. One way for relaxing this specification is to decrease the distance between the exit pupil and the focal plane. An alternative design has shown that this distance could be reduced down to 4700 mm, leading to an angular resolution of 140 nrad. A range of ±30 pixels, mainly driven by AOCS low frequency drifting, corresponds to an amplitude of 42 μrad. These requirements are roughly in agreement with the features of the FSM developed by Gigan [1].

3.3 Performance analysis of the closed-loop control

The closed-loop control can efficiently damp vibrations up to the limit frequency, which strongly depends on the sample frequency. The sample frequency, which is necessarily lower than the measurement frequency, is here chosen equal to the measurement frequency. We can estimate the limit frequency as approximately a fifth of the measurement frequency, depending on the efficiency of the controller.

Let us analyse the performances of the closed-loop control in the two previous examples.

▪ **with the 16 m mono-pupil**, preliminary studies show that the limit frequency is greater than 150 Hz, which is greater than the highest frequency sinusoidal vibration. In this hypothetical case, the required accuracy is obtained whatever the integration time.

▪ **With the 9-pupil OAS system** and a measurement frequency of around 220 Hz, preliminary studies show that the limit frequency is about 50-60 Hz. Owing to our μ-vibrations PSD hypothesis, despite of this limit frequency, the closed-loop control enables to increase significantly the required elementary integration time for the post-accumulation by a factor 3 to 6. Consequently, the required number of elementary acquisitions is between 20 to 40 instead of 800 when the line of sight is uncontrolled (*c.f.* Fig. 3). Thus, the closed-loop control saves a considerable amount of required acquisitions for the post-accumulation (ratio between 20 and 40).

4. CONCLUSION

Controlling the line of sight μ-vibrations is one of the *sine qua non* condition of the high resolution Earth observation from high orbits.

On the one hand, post-accumulation processing can be a solution provided that the elementary integration time is not too short. Otherwise, the huge amount of data and the very long global integration time are prohibitive.

On the second hand, the closed-loop control is able to attenuate μ-vibrations up to a limit frequency. This limit frequency is proportional to the measurement frequency of the μ-vibrations sensor in a typical ratio of 1 to 5, depending of the controller's efficiency. The measurement frequency is mainly limited by the sensor integration time to achieve the required accuracy. This integration time is all more long as the OAS system is diluted, due to its small collecting area and the faintness of its OTF's modulus.

In the case of the 9-pupil OAS system, the use of the closed-loop control enables to decrease the huge number of required elementary acquisitions for post-accumulation from 800 to an acceptable one, between 20 and 40.

As a conclusion, closed-loop stabilisation control and post-accumulation are two complementary means for the line of sight μ-vibrations damping strategy.

5. REFERENCES

1. Arsenault R., Donaldson R. , Dupuy C ., Fedrigo E., Hubin N. , Ivanescu L. , Kasper M. , Oberti, S. , Paufique J. , Rossi S. , Silber A. , Delabre B. , Lizon J.L. , Gigan P. , 2004. *MACAO-VLTI adaptive optics systems performance*. SPIE, Vol. 5490, pp. 47-58.
2. Blanc P., Thomas E., Falzon F., 2004. *Imagerie de la Terre à Haute Résolution par Synthèse d'Ouverture Optique*. Bulletin Bibliographique POLOQ, Délégation Générale pour l'Armement, Groupe de Prospective Orientée sur les Lasers et l'OptroniqQue, DGA/D4S/MRIS.
3. Blanc P. 1999. *Développement de méthodes pour la détection de changement*. Science Doctorate Thesis. Ecole des Mines de Paris, France, 227 pp.
4. Mesrine M., Thomas E., Garin S., Blanc P., Alis C., Cassaing F., Laubier D., 2006. High resolution Earth Observation from Geostationary Orbit by optical aperture synthesis. *In proceedings of the '6th International Conference on Space Optics*, ESTEC, Noordwijk, The Netherlands, 27-30 June 2006.
5. Thomas E., Blanc P., Falzon F., 2005. A new concept of synthetic aperture instrument for high resolution Earth observation from high orbits. *In : proceedings of the Symposium Disruption in Space*, Marseille, France, 4-6 july.
6. Pratt, W. K., 1991. *Digital image processing (second edition)*, John Wiley & Sons Inc., New York, USA, ISBN 0-521-43108-5, 970 pp.
7. Stern, A., Kopeika, N.S., 1997. Analytical method to calculate optical transfer functions for image motion and vibrations using moments. J. Opt. Soc. Am. A. Vol. 14, No. 2.